

Mitochondria-targeting properties and photodynamic activities of porphyrin derivatives bearing cationic pendant

Wanhua Lei, Jingfan Xie, Yuanjun Hou, Guoyu Jiang, Hongyan Zhang, Pengfei Wang, Xuesong Wang*, Baowen Zhang

Key Laboratory of Photochemical Conversion and Optoelectronic Materials, Technical Institute of Physics and Chemistry, Chinese Academy of Sciences, Beijing 100190, PR China

ARTICLE INFO

Article history:

Received 24 June 2009

Received in revised form 8 December 2009

Accepted 14 December 2009

Available online 22 December 2009

Keywords:

Photodynamic therapy

Mitochondria-targeting

Lipophilic cation

ABSTRACT

Four *meso*-tetraphenylporphyrin derivatives bearing either triphenylphosphonium ion-(**P1** and **P2**) or triethylammonium ion-(**P3** and **P4**) terminated alkoxy group at either *para*-(**P1** and **P3**) or *meta*-(**P2** and **P4**) position of one *meso*-phenyl group were designed and synthesized. **P1–P4** show similar absorption and fluorescence emission spectra and $^1\text{O}_2$ quantum yields. The more lipophilic nature of triphenylphosphonium ion over triethylammonium ion renders **P1** and **P2** higher octanol/water partition coefficients than **P3** and **P4**. Confocal fluorescence microscopy proved that **P1–P4** are all mitochondria-targeting. MTT assay showed that **P1–P4** presented significant phototoxicity at the concentrations that dark toxicity is negligible towards human breast cancer cell line MCF-7 cells, displaying their application potential in PDT.

© 2009 Elsevier B.V. All rights reserved.

1. Introduction

Photodynamic therapy (PDT) is a novel treatment modality for numerous cancers and certain noncancerous diseases [1]. It utilizes the photoreactions mediated by photosensitizer, light, and oxygen to generate reactive oxygen species (ROS), such as singlet oxygen ($^1\text{O}_2$), superoxide anion radical (O_2^-), and hydroxyl radical ($\cdot\text{OH}$), and relies on the cytotoxic effects of ROS to lead to apoptosis or necrosis of abnormal cells. The short lifetime and thus the very limited diffusion distance of ROS in biological systems, for example, the diffusion range of $^1\text{O}_2$ is smaller than 0.1 μm in tissues, render PDT “in situ” character, i.e. the site of photodamage is also the site where ROS is generated [2]. Consequently, the PDT efficacy is dependent not only on the selective accumulation but also on the subcellular localization of photosensitizers in abnormal cells. In this regard, mitochondria-targeting is of importance for PDT due to its key role in regulating apoptotic cell death [3]. So far two major apoptotic pathways have been characterized: the death receptor-mediated, or extrinsic pathway, and the mitochondria-mediated apoptosis, or intrinsic pathway [4,5]. The central place of mitochondria as regulators of apoptotic cell death has stimulated great interest in developing mitochondria-targeting chemotherapy [6–9]. In the field of PDT, some photosensitizers, such as protoporphyrin IX [10,11] and phthalocyanine Pc4 [12,13], have been known mitochondria localization for a long time, and photosensitizers that

localize to mitochondria are reported to be more efficient in killing cells than those that localize at other cellular sites [14–16]. However, preparing mitochondria-targeting PDT photosensitizers by rational molecular design is still in its infancy [17–19]. Two strategies are widely used to render biologically active molecules mitochondria-targeting capability: (1) tethering a mitochondrial localization peptide sequence, which utilizes protein import pathway; and (2) attaching a lipophilic cation group, which utilizes the high membrane potential (-180 mV) across the inner mitochondrial membrane [20]. Recently, Asayama et al. [17] used a peptide modified Mn-porphyrin to target mitochondria, Vicente and co-workers [18] synthesized a series of amphiphilic cationic porphyrin derivatives bearing either a group with positive charge (guanidinium or biguanidinium) or a mitochondrial localization peptide, and Kopeček and co-workers [19] targeted a HPMA copolymer-bound Mce6 to mitochondria by grafting triphenylphosphonium ion. Though there are a number of lipophilic cations can be chosen, triphenylphosphonium ion is particularly unique for mitochondria targeting, mainly due to its simplicity in structure and ease to be linked on the target molecules. Thus, triphenylphosphonium ion-based compound class includes the majority of the non-peptidic mitochondrial targeting agents synthesized to date [20]. So far, only one example of triphenylphosphonium ion-modified PDT photosensitizer was reported [19], in which the complicated synthesis hindered in depth studies, such as the influence of linking modes between porphyrin derivatives and triphenylphosphonium ion and further structural optimization for PDT efficacy improvement. In this work, four cation ion-modified *meso*-tetraphenylporphyrin

* Corresponding author. Tel.: +86 10 8254 3592; fax: +86 10 6255 4670.
E-mail addresses: g203@mail.ipc.ac.cn, xswang@mail.ipc.ac.cn (X. Wang).

derivatives (**P1–P4**) were synthesized through a facile way, two of them (**P1** and **P2**) are based on triphenylphosphonium ion and the other two (**P3** and **P4**) triethylammonium ion, and the cation pendant is anchored on the phenyl group at either *para*- or *meta*-position (Scheme 1). All the four porphyrins were found to specifically localize in mitochondria of MCF-7 cells and show good photo-dynamic activities. In particular, **P1** presents the highest cellular uptake and the lowest dark toxicity among the four compounds, implying the important role of modification mode. The results suggest that PDT efficacy may be further improved via delicate design of the linking mode of the lipophilic cation group to porphyrin-based chromophores. Moreover, easy preparation method adopted in our work make the structural optimization convenient.

2. Material and methods

2.1. Synthesis

The mixture of 0.2 g of 5-(4-hydroxy-phenyl)-10,15,20-triphenylporphyrin, 1.5 g of anhydrous K_2CO_3 , and 15 mL of 1,4-dibromobutane was heated at 150 °C for 2 h under N_2 atmosphere. After removal of 1,4-dibromobutane in vacuum, the residue was extracted with chloroform and the extract was subjected to column chromatography on silica gel using chloroform 5-(*p*-(4-bromo)-butoxyphenyl)-10,15,20-triphenylporphyrin in yield of 87%. The obtained product was mixed with excess triphenylphosphine and heated at 100 °C for 14 h under N_2 atmosphere. After cooling to room temperature, chloroform was added to dissolve the solid. Column chromatography of the chloroform solution on silica gel using chloroform/petroleum ether (50/50) as eluent removed triphenylphosphine at first and then the use of chloroform/methanol (93:7) as eluent gave the target photosensitizer **P1** in yield of 74%. Similar procedures were used to prepare **P2–P4**, all in similar good yields.

5-(*p*-(4-triphenylphosphonium)-butoxyphenyl)-10,15,20-triphenylporphyrin bromide (**P1**). 1H NMR (400 MHz, in $CDCl_3$): δ = -2.77 (s, 2H), 2.00–2.08 (bs, 2H), 2.40–2.60 (bs, 2H), 4.10–4.30 (m, 2H), 4.39 (bs, 2H), 7.19–7.22 (d, 2H, J = 8.0 Hz), 7.74–7.81 (m, 18H), 7.93–7.98 (m, 6H), 8.08–8.10 (d, 2H, J = 8.0 Hz),

8.20–8.22 (d, 6H, J = 6.4 Hz), 8.84 (bs, 8H). ESI-MS: m/z = 947.5 ($[M-Br]^+$).

5-(*m*-(4-triphenylphosphonium)-butoxyphenyl)-10,15,20-triphenylporphyrin bromide (**P2**). 1H NMR (400 MHz, in $CDCl_3$): δ = -2.79 (s, 2H), 1.93–1.95 (m, 2H), 2.30–2.33 (m, 2H), 4.00 (m, 2H), 4.28–4.31 (t, 2H, J = 5.5 Hz), 7.28–7.30 (d, 1H), 7.53–7.65 (m, 11H), 7.74–7.83 (m, 16H), 8.20–8.22 (d, 6H, J = 5.4 Hz), 8.82–8.85 (m, 8H). ESI-MS: m/z = 947.5 ($[M-Br]^+$).

5-(*p*-(4-triethylammonium)-butoxyphenyl)-10,15,20-triphenylporphyrin bromide (**P3**). 1H NMR (400 MHz, in $CDCl_3$): δ = -2.77 (s, 2H), 1.19–1.23 (t, 9H, J = 14.0 Hz), 2.00–2.20 (bs, 4H), 3.40–3.70 (bs, 8H), 4.33 (bs, 2H), 7.25–7.27 (d, 2H, mixed with $CHCl_3$), 7.72–7.78 (m, 9H), 8.11–8.13 (d, 2H, J = 6.7 Hz), 8.20–8.22 (d, 6H, J = 6.6 Hz), 8.84–8.85 (bs, 8H). ESI-MS: m/z = 786.5 ($[M-Br]^+$).

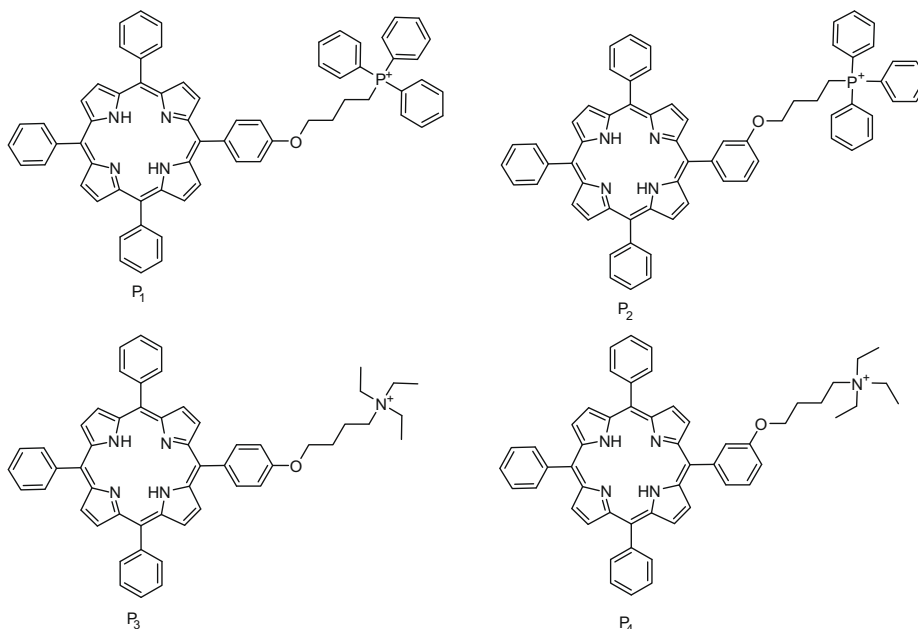
5-(*m*-(4-triethylammonium)-butoxyphenyl)-10,15,20-triphenylporphyrin bromide (**P4**). 1H NMR (400 MHz, in $CDCl_3$): δ = -2.80 (s, 2H), 1.11–1.13 (t, 9H, J = 14.2 Hz), 1.86–1.89 (m, 4H), 3.05–3.08 (m, 6H), 3.14–3.20 (m, 2H), 4.16–4.18 (t, 2H, J = 5.4 Hz), 7.62 (t, 1H, J = 8.0 Hz), 7.68 (bs, 1H), 7.83 (d, 1H, J = 8.0 Hz), 8.19–8.21 (d, 6H, J = 5.8 Hz), 8.84–8.87 (m, 8H). ESI-MS: m/z = 786.5 ($[M-Br]^+$).

2.2. Singlet oxygen quantum yields [21]

A series of 2 mL of air-saturated acetonitrile solutions containing 1,3-diphenylisobenzofuran (DPBF, 20 μ M) and the examined photosensitizer, of which the absorbance at 512 nm originating from the absorption of the photosensitizer was adjusted to the same (OD = 0.15), were separately charged into an opened 1 cm path fluorescence cuvette and illuminated with light of 512 nm (obtained from a Hitachi F-4500 Fluorescence Spectrophotometer). The consumptions of DPBF were followed by monitoring its fluorescence intensity decrease at the emission maximum (λ_{ex} = 445 nm) at different irradiation time. *Meso*-tetraphenylporphyrin (TPP) was used as standard, whose 1O_2 quantum yield was determined to be 0.60 in air-saturated acetonitrile [22,23].

2.3. *n*-Octanol/water partition coefficients (log *P*)

Typically, a solution of photosensitizer (50 μ M) in equal volumes of 50 μ M PBS, pH 7.4 (1 mL) and 1-octanol (1 mL) was sonicated for 30 min. After separation by centrifugation, 20 μ L of



Scheme 1. Structures of the examined photosensitizers **P1–P4** (all isolated as bromide salts).

1-octanol phase and 100 μL of water phase were taken and diluted by DMSO to 2 mL and 1 mL, respectively. The amounts of the photosensitizer in each phase were determined by monitoring fluorescence intensity at 655 nm (418 nm excitation) on a Hitachi F-4500 Fluorescence Spectrophotometer. The results are the average of three independent measurements.

2.4. Cell culture

All tissue culture media and reagents were obtained from HyClone, Thermo Scientific. MCF-7 cells were maintained in DMEM containing 10% fetal bovine serum.

2.5. Cellular uptake

MCF-7 cells were plated at 2×10^5 per well in a Nunc 48 well plate and allowed to grow for 24 h. Photosensitizer stocks were prepared in DMSO at the concentration of 1 mM and then diluted into medium to the final working concentrations (the final concentration of DMSO was less than 5%). The cells were exposed to 10 μM of photosensitizer for 0, 1, 2, and 4 h, respectively. At the end of the incubation time, the loading medium was removed and the cells were washed with 500 μL of PBS three times. The cells were solubilized upon addition of 500 μL of 0.25% Triton X-100 in PBS. Fluorescence emission intensities at 655 nm (418 nm excitation) were measured to determine the porphyrin concentration that taken up, on a Hitachi F-4500 Fluorescence Spectrophotometer.

2.6. Subcellular localization

The MCF-7 cells were plated on Culture Dishes containing a microscope slide for confocal laser scanning microscopy (CLSM) observations. For the colocalization experiments the cells were incubated concurrently with 10 μM of photosensitizer and 10 μM of Rhodamine 123 for 4 h. Then the slides were washed three times with 5 mM PBS pH 7.4. Fluorescent microscopy was performed using a Nikon C1Si inverted fluorescent microscope and the magnification employed was 10×60 .

2.7. Dark cytotoxicity

The MCF-7 cells were plated as described above and allowed 24 h to attach. The cells were exposed to increasing concentrations of photosensitizer up to 50 μM and incubated for 24 h. The loading medium was then removed and the cells were fed with medium containing MTT from Sigma. Cell viability was then measured by reading the absorbance at 570 nm using a Thermo MK3 Multiscan microplate reader. The signal was normalized to 100% viable (untreated) cells.

2.8. Phototoxicity

The MCF-7 cells were prepared as described above and treated with photosensitizer at the concentrations of 0, 1, 2, 4, 6, 8, and 10 μM , respectively. The cells were then exposed to light >550 nm (using an Oriel 91192 Solar simulator as light source and a 550 nm cut-off filter to remove the short wavelength light) for 30 min. The irradiation intensity was about 14 mW/cm^2 and the total light dose was approximately 25 J/cm^2 . The cells were returned to the incubator overnight and assayed for viability as described above.

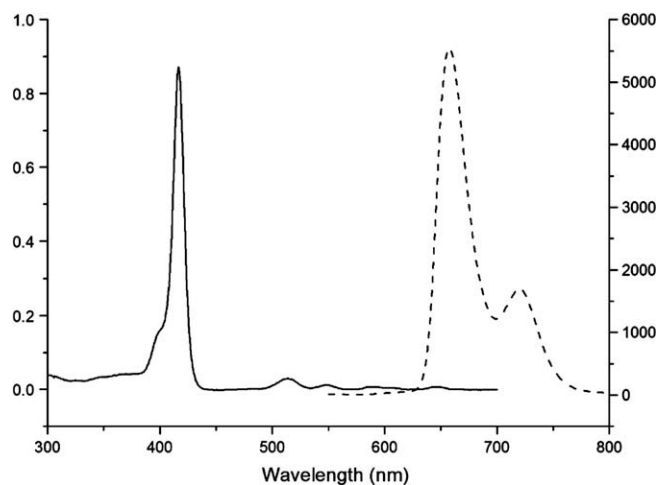


Fig. 1. Absorption (solid line) and fluorescence emission (dash line, $\lambda_{\text{ex}} = 420$ nm) spectra of **P1** in DMSO.

3. Results and discussion

3.1. Photophysical and photochemical properties

As expected, the four porphyrin derivatives exhibit nearly identical photophysical properties due to their high similarity in chemical structures. Fig. 1 shows the absorption spectrum and fluorescence emission spectrum of **P1** in DMSO, in which one strong Soret band, four less intense Q bands, as well as an emission band with fine structures are observed, all typical for porphyrins [24,25]. Similar absorption and fluorescence spectra were obtained for **P2–P3**. The absorption maxima of the Soret bands and the emission maxima of **P1–P4** were collected in Table 1. The marginal spectrum red shift (about 1 nm) for **P1** versus **P2** or for **P3** versus **P4** originates from the substitution of alkoxy group at the different positions (*para*- versus *meta*-) of the phenyl group.

Singlet oxygen quantum yields of **P1–P4** in acetonitrile were determined using 1,3-diphenylisobenzofuran (DPBF) as the chemical trap of $^1\text{O}_2$ [21], which does not fluoresce upon oxidation by $^1\text{O}_2$, and *meso*-tetraphenylporphyrin (TPP) as reference [22,23], whose $^1\text{O}_2$ quantum yield in acetonitrile was measured to be 0.6. Fig. 2 gives the DPBF fluorescence intensity as the function of irradiation time. The fluorescence quenching rates are proportional to the $^1\text{O}_2$ quantum yields of the photosensitizers. Thus, the $^1\text{O}_2$ quantum yields of **P1–P4** were measured to be 0.53, 0.50, 0.57, and 0.58, respectively. Obviously, **P1–P4** can generate $^1\text{O}_2$ as efficiently as their parent molecule TPP, and therefore are expected to be effective PDT agents.

Though the porphyrins bearing either triphenylphosphonium ion or triethylammonium ion exhibit similar absorption spectra as well as $^1\text{O}_2$ quantum yields, their amphiphilicity, a property also

Table 1

Absorption and emission maxima, $^1\text{O}_2$ quantum yields, and *n*-octanol/water partition coefficients ($\log P$) for **P1–P4**.

Porphyryns	P1	P2	P3	P4
$\lambda_{\text{max}}^{\text{ab}}$ (nm) ^a	420	419	420	419
$\lambda_{\text{max}}^{\text{em}}$ (nm) ^b	658	657	657	656
$(\phi^1\text{O}_2)^{\text{c}}$	0.53	0.50	0.57	0.58
$\log P^{\text{d}}$	1.57	1.87	0.73	0.84

^a Absorption maximum in DMSO.

^b Fluorescence emission maximum in DMSO.

^c $^1\text{O}_2$ quantum yield in acetonitrile, using TPP as reference (0.60).

^d SD < 5%.

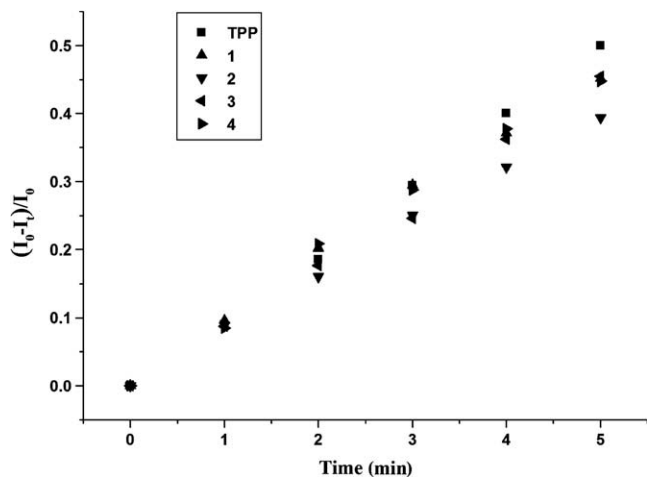


Fig. 2. DPBF consumption as a function of irradiation time in air-equilibrated CH_3CN solutions of TPP (Square), **P1** (up triangle), **P2** (down triangle), **P3** (left triangle), and **P4** (right triangle). I_0 and I_t are, respectively, the fluorescence intensities before and after irradiation.

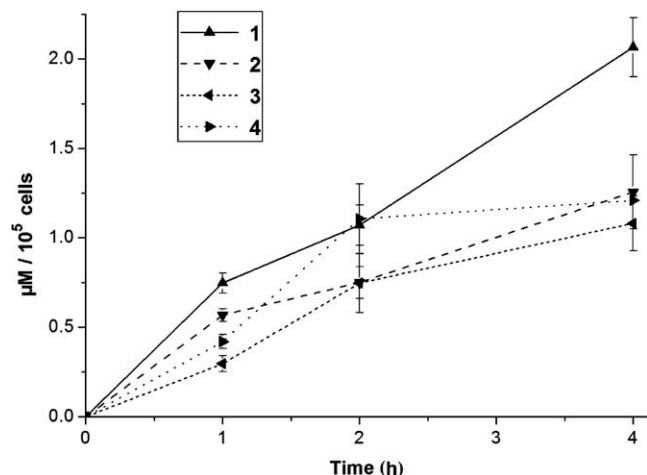


Fig. 3. Time-dependent uptake of **P1** (up triangle), **P2** (down triangle), **P3** (left triangle), and **P4** (right triangle) at $10 \mu\text{M}$ by MCF-7 cells.

important for PDT [26,27], presents large differences. Table 1 shows the octanol/water partition coefficients of **P1–P4** measured with pH 7.4 PBS ($5 \mu\text{M}$) as the aqueous phase. While $\text{Log } P$ values of **P1** and **P2** are 1.57 and 1.87, the values for **P3** and **P4** are only 0.73 and 0.84, indicating somewhat stronger hydrophilic feature of **P3** and **P4** than **P1** and **P2**. The result demonstrates that triphenylphosphonium ion is a more lipophilic cation ion than its counterpart triethylammonium ion. Moreover, a little bit higher lipophilic char-

acter of **P2** than **P1** as well as **P4** than **P3** suggests that substitution position of cationic pendant on the phenyl group of porphyrins also play a delicate role in the amphiphilicity.

3.2. Cellular uptake

The time-dependent cellular uptake of **P1–P4** was evaluated in human breast cancer cell line MCF-7 at a concentration of $10 \mu\text{M}$, and the results are shown in Fig. 3. **P3** and **P4**, bearing triethylammonium ion-based pendant, exhibit lower cell uptake than **P1** after 4 h incubation. Because the process of partitioning has not reached equilibrium during 4 h, the differences in cellular uptake are most likely related to kinetics of binding rather than to the extent of binding. The observed faster cellular uptake of **P1** may presumably attributed to its higher lipophilic character, which facilitates it to penetrate into the bilayer membrane of cells [26,27].

Interestingly, **P2**, which is more lipophilic than **P1**, was taken up just in the same amount as **P3** and **P4**, nearly half of that of **P1**.

3.3. Subcellular localization

The four cationic porphyrins **P1–P4** show similar fluorescence patterns in MCF-7 cells when investigated by confocal fluorescence microscopy. Fig. 4 shows the confocal micrographs of the double-stained MCF-7 cells with **P1** and a mitochondria specific fluorescent probe Rhodamine 123 [20]. When excited at 405 nm, red fluorescence attributable to **P1** emission was observed (left panel in Fig. 4), while 488 nm of excitation gave rise to typical green fluorescence of Rhodamine 123 (middle panel). Their overlapping images exhibited an orange color (right panel). A perfect superposition between the Rhodamine dye image and that of **P1** is evident, proving the subcellular localization of **P1** in mitochondria. This was expected since both dyes are lipophilic cations, and thus have a preference for mitochondrial organelle, driven by the extra large membrane potential across the inner mitochondrial membrane. The same subcellular localization was also confirmed for **P2–P4**.

3.4. Cytotoxicity and phototoxicity

The dark cytotoxicity of the four porphyrins **P1–P4** were evaluated in MCF-7 cells by exposure to increasing amount of each porphyrin derivative for 24 h, and cell survival was determined by MTT assay (Fig. 5). None of **P1–P4** displayed significant dark cytotoxicity up to a concentration of $10 \mu\text{M}$. The cytotoxicity emerged clearly at the concentrations higher than $10 \mu\text{M}$. **P3** and **P4** with triethylammonium ion pendant are significantly more cytotoxic than **P1** and **P2** that bear triphenylphosphonium ion pendant. It is worth to note that **P1**, which possesses the highest cell uptake among the four porphyrins, show the least dark cytotoxicity. For example, at $25 \mu\text{M}$, cell survival of **P1** treated cells was 65%, in sharp contrast to the case of **P4**, where the cell viability was only

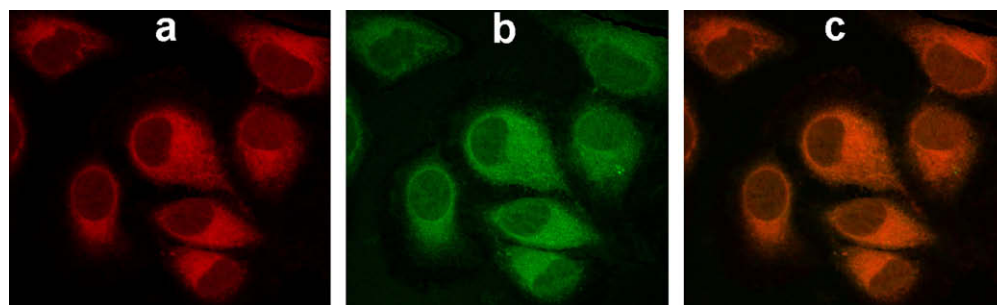


Fig. 4. Confocal micrographs of the double-stained MCF-7 cells with **P1** and Rhodamine 123 (each $10 \mu\text{M}$ incubated for 4 h). (a) **P1** fluorescence image upon excitation at 405 nm, (b) Rhodamine 123 fluorescence image upon excitation at 488 nm, (c) overlay of the former two fluorescence images.

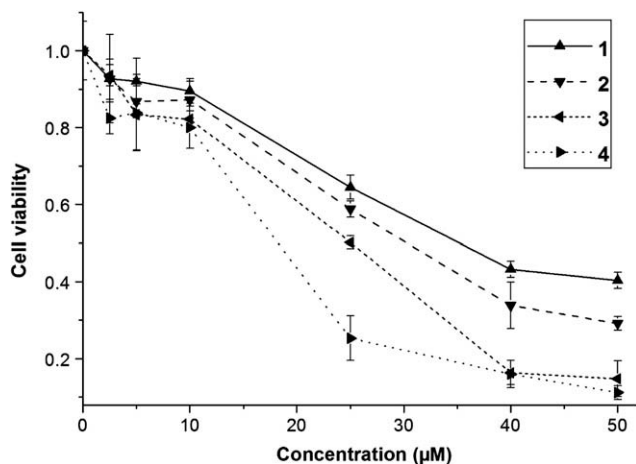


Fig. 5. Dark toxicity of **P1** (up triangle), **P2** (down triangle), **P3** (left triangle), and **P4** (right triangle) at varied concentrations toward MCF-7 cells using MTT assay.

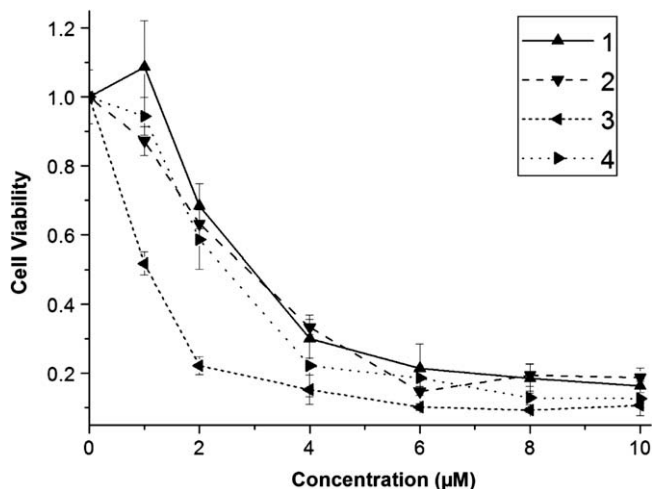


Fig. 6. Phototoxicity of **P1** (up triangle), **P2** (down triangle), **P3** (left triangle), and **P4** (right triangle) at varied concentrations toward MCF-7 cells using MTT assay.

25%. The dark cytotoxicity follows the order of **P4** > **P3** > **P2** > **P1** at the examined concentrations.

For phototoxicity study, cultured cells were incubated for 4 h in the dark with various concentrations of photosensitizer and then irradiated with broadband light (>550 nm) for 30 min. After irradiation, the cells were incubated for another 19.5 h and then subjected to cell survival analysis. Photosensitizer-free controls (i.e. similar procedures except that no photosensitizer was added) were also carried out. The data presented in Fig. 6 demonstrate that **P3** photodamage MCF-7 cells with somewhat higher efficiency among the four porphyrins. Under the concentration of 2 µM, **P3** reduced cell viability by 80%, while the other three porphyrins gave a 30–40% reduction in cell viability. At the concentrations equal to or larger than 6 µM, the four porphyrins showed similarly effective phototoxicity, indicating their potential in PDT.

4. Conclusions

In summary, four *meso*-tetraphenylporphyrin derivatives bearing either triphenylphosphonium ion (**P1** and **P2**) or triethylammonium ion (**P3** and **P4**) terminated alkoxy group at either *para*- (**P1** and **P3**) or *meta*- (**P2** and **P4**) position of one *meso*-phenyl group were designed and synthesized. It was found that **P1–P4** show similar absorption and fluorescence emission spectra, $^1\text{O}_2$

quantum yields, as well as mitochondria-targeting property. **P1** exhibits the least dark cytotoxicity and **P3** possesses the highest phototoxicity among the four porphyrins, both toward MCF-7 cells. Importantly, all of them present significant phototoxicity but negligible dark toxicity at the concentrations 6–10 µM, displaying their potential in PDT.

Acknowledgement

This work was financially supported by NNSFC (20772133, 20873170) and CAS (KJCX2.YW.H08).

References

- [1] M.R. Detty, S.L. Gibson, S.J. Wagner, Current clinical and preclinical photosensitizers for use in photodynamic therapy, *J. Med. Chem.* 47 (2004) 3897–3915.
- [2] M. Sibirian-Vazquez, T.J. Jensen, M.G.H. Vicente, Porphyrin–retinamides: synthesis and cellular studies, *Bioconjugate Chem.* 18 (2007) 1185–1193.
- [3] N.L. Oleinick, R.L. Morris, I. Belichenko, The role of apoptosis in response to photodynamic therapy: what, where, why, and how, *Photochem. Photobiol. Sci.* 1 (2002) 1–21.
- [4] Y. Shi, A structural view of mitochondria-mediated apoptosis, *Nat. Struct. Biol.* 8 (2001) 394–401.
- [5] R.D. Almeida, B.T. Manadas, A.P. Carvalho, C.B. Duarte, Intracellular signaling mechanisms in photodynamic therapy, *Biochim. Biophys. Acta* 1704 (2004) 59–86.
- [6] J.L. Hickey, R.A. Ruhayel, P.J. Barnard, M.V. Baker, S.J. Berners-Price, A. Filipovska, Mitochondria-targeted chemotherapeutics: the rational design of gold(I) N-heterocyclic carbene complexes that are selectively toxic to cancer cells and target protein selenols in preference to thiols, *J. Am. Chem. Soc.* 130 (2008) 12570–12571.
- [7] D.R. Green, G. Kroemer, The pathophysiology of mitochondrial cell death, *Science* 305 (2004) 626–629.
- [8] L. Galluzzi, N. Larochette, N. Zamzami, G. Kroemer, Mitochondria as therapeutic targets for cancer chemotherapy, *Oncogene* 25 (2006) 4812–4830.
- [9] V.R. Fantin, P. Leder, Mitochondriotoxic compounds for cancer therapy, *Oncogene* 25 (2006) 4787–4797.
- [10] A. Verma, J. Nye, S.H. Snyder, Porphyrins are endogenous ligands for the mitochondrial (peripheral-type) benzodiazepine receptor, *Proc. Natl. Acad. Sci. USA* 84 (1987) 2256–2260.
- [11] A. Verma, S.L. Facchina, D.J. Hirsch, S.Y. Song, L.F. Dillahey, J.R. Williams, S.H. Snyder, Photodynamic tumor therapy: mitochondrial benzodiazepine receptors as a therapeutic target, *Mol. Med.* 4 (1998) 40–45.
- [12] J. Morgan, A.R. Oseroff, Mitochondria-based photodynamic anti-cancer therapy, *Adv. Drug Delivery Rev.* 49 (2001) 71–86.
- [13] N.S. Trivedi, H.W. Wang, A.L. Nieminen, N.L. Oleinick, J.A. Izatt, Quantitative analysis of Pc 4 localization in mouse lymphoma (LY-R) cells via double-label confocal fluorescence microscopy, *Photochem. Photobiol.* 71 (2000) 634–639.
- [14] D. Kessel, Y. Luo, Mitochondrial photodamage and PDT-induced apoptosis, *J. Photochem. Photobiol. B: Biol.* 42 (1998) 89–95.
- [15] D. Kessel, Y. Luo, Y. Deng, C.K. Chang, The role of subcellular localization in initiation of apoptosis by photodynamic therapy, *Photochem. Photobiol.* 65 (1997) 422–426.
- [16] D. Kessel, Y. Luo, Photodynamic therapy: a mitochondrial inducer of apoptosis, *Cell Death Differ.* 6 (1999) 28–35.
- [17] S. Asayama, E. Kawamura, S. Nagaoka, H. Kawakami, Design of manganese porphyrin modified with mitochondrial signal peptide for a new antioxidant, *Mol. Pharm.* 3 (2006) 468–470.
- [18] M. Sibirian-Vazquez, I.V. Nesterova, T.J. Jensen, M.G.H. Vicente, Mitochondria targeting by guanidine- and biguanidine-porphyrin photosensitizers, *Bioconjugate Chem.* 19 (2008) 705–713.
- [19] V. Cuchelkar, P. Kopečková, J. Kopeček, Novel HPMA copolymer-bound constructs for combined tumor and mitochondrial targeting, *Mol. Pharm.* 5 (2008) 776–786.
- [20] A.T. Hoye, J.E. Davoren, P. Wipf, M.P. Fink, V.E. Kagan, Targeting mitochondria, *Acc. Chem. Res.* 41 (2008) 87.
- [21] R.H. Young, K. Wehrly, R.L. Martin, Solvent effects in dye-sensitized photooxidation reactions, *J. Am. Chem. Soc.* 93 (1971) 5774–5779.
- [22] F. Wilkinson, Quantum yields for the photosensitized formation of the lowest electronically excited singlet state of molecular oxygen in solution, *J. Phys. Chem. Ref. Data* 22 (1993) 113–262.
- [23] R.W. Redmond, J.N. Gamlin, A compilation of singlet oxygen yields from biologically relevant molecules, *Photochem. Photobiol.* 70 (1999) 391–475.
- [24] M. Gouterman, Spectra of porphyrins, *J. Mol. Spectrosc.* 6 (1961) 138–163.
- [25] M. Gouterman, G.H. Wagniere, L.C. Snyder, Spectra of porphyrins part II. Four orbital model, *J. Mol. Spectrosc.* 11 (1963) 108–127.
- [26] T.J. Dougherty, Photosensitizers: therapy and detection of malignant tumors, *Photochem. Photobiol.* 45 (1987) 879–889.
- [27] R.W. Boyle, D. Dolphin, Structure and biodistribution relationships of photodynamic sensitizers, *Photochem. Photobiol.* 64 (1996) 469–485.